TID-4500, UC-34
Physics, General

LAWRENCE LIVERMORE LABORATORY
University of California/Livermore, California/94550

UCRL-51479

MEASUREMENT OF EARTH MEDIUM ELECTRICAL CHARACTERISTICS: TECHNIQUES , RESULTS, AND APPLICATIONS

R. Jeffrey Lytle

MS. date: November 12, 1973

DISCLAIMER

Foreword

This report expands upon the material presented in an invited paper at the Workshop on Radio Systems in Forrested and/or Vegetated Environments, held by the United States Army Communication Command at Fort Huachuca, Arizona, November 1973. The survey of work in the area of earth medium electrical parameter measurements, results and applications is not exhaustive, but only representative of the subject matter. Nevertheless, the account given here should provide the reader with an overview of basic methods, results and applications in this area.

Contents

MEASUREMENT OF EARTH MEDIUM ELECTRICAL CHARACTERISTICS: TECHNIQUES, RESULTS, AND APPLICATIONS

Abstract

An overview of measurement techniques, measurement results, and factors influencing the conductivity and dielectric constant of earth medium is given. Application of these measurement techniques to geophysical investigations is also discussed.

Introduction

The earth electrical conductivity σ and dielectric constant ϵ can have a decided effect upon the performance of electromagnetic systems (e.g., communication systems and geophysical probing systems). These parameters influence the choice of antenna, the antenna efficiency, whether a ground screen is needed and its size, the transmission loss and phase shift, the dominant path of propagation, the effect of dispersion, hardening considerations, the relative communication efficiency, and environmental effects, among other factors. Values of σ and ϵ for a wide number of environments are hence needed in theoretical assessments of system utility.

Examples of laboratory and in situ methods of determining σ and ϵ are given in this report. The in situ methods include both surface and drill hole procedures. Some references describing various methods are given; however, the reference list is not to be considered definitive. There are numerous other references describing these procedures which are not listed herein. For general background information, a list of overview references[1-17] concerned with electrical probing of the earth (with particular emphasis on methods of measuring σ and ϵ and results for σ and ϵ) are presented. References pertaining to specific measurement schemes and applications[18-79] are also given. There are of course alternative measurement schemes which are not mentioned herein. The list of measurement techniques is however thought to be representative of the more commonly used procedures.

The electrical constitutive parameters σ and ϵ depend upon frequency, water content, temperature, geological constituents, weathering factors, local anomalies, and other considerations. Due to the myriad factors influencing σ and ϵ, it is preferable to perform in situ measurements of σ and ϵ, rather than perform laboratory measurements on "representative samples" or to rely on "textbook values." Hence, in situ measurement schemes, rather than laboratory

measurement schemes or "nominal values" for σ and ϵ, are stressed in this summary.

In situ measurement schemes have the potential of probing the near surface, as well as greater depths. These techniques thus can be used for detecting buried objects, faults, and discontinuities, in addition to determining the ground parameters. For example, these methods have been used to determine the location of plastic and metallic pipes, the depth of the water table, the location of gravel deposits, identifying mineral nodule deposits on the ocean floor, determining glacial ice depth, defining geothermal areas, mapping the boundaries of buried salt domes, and locating underground chambers. In many situations, large propagation losses or severe data inversion requirements preclude successfully determining a detailed subsurface profile of σ and ϵ. Nevertheless, in situ measurement schemes and data inversion methods do hold great promise in geology, hydrology, mining, archaeology exploration, and location of energy resources and definition of their extent, among others.

Laboratory Measurements

BRIDGE METHODS

A parallel-plate capacitor is commonly used to hold the right circular disc sample of the material. Two terminal holders (see Fig. 1) are commonly used. This method has been used for frequencies of 10^{-2} to 10^{9} Hz. Procedures exist for accounting for the inductance and conductance of the connecting leads. Much care has to be taken to insure a good contact between the sample and the electrodes. Substitution techniques with liquid immersion of the sample enable one to attain high accuracy for the loss tangent. (See Refs. 10, 14, 16, 18, 19, 21, 22, 26, 27, 62.)

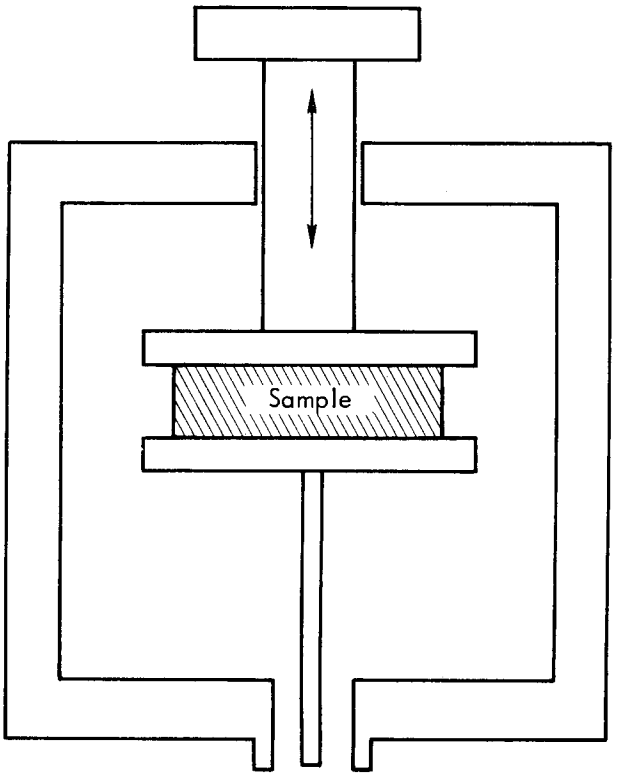

Fig. 1. A Hartshorn-Ward capacitive holder. Upper electrode is micrometer-driven.

TRANSMISSION LINE METHODS

A short-circuited transmission line with the sample at the end of the line (see Fig. 2) enables one to use standard impedance transformation formulae to

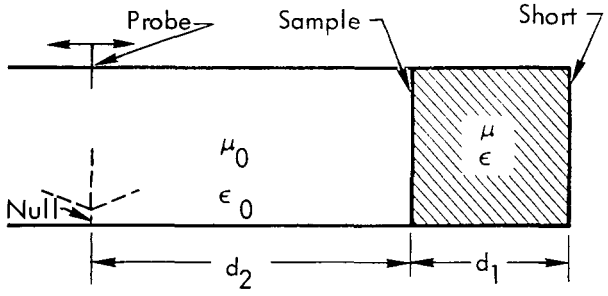

Fig. 2. Sample in shorted line with traveling probe.

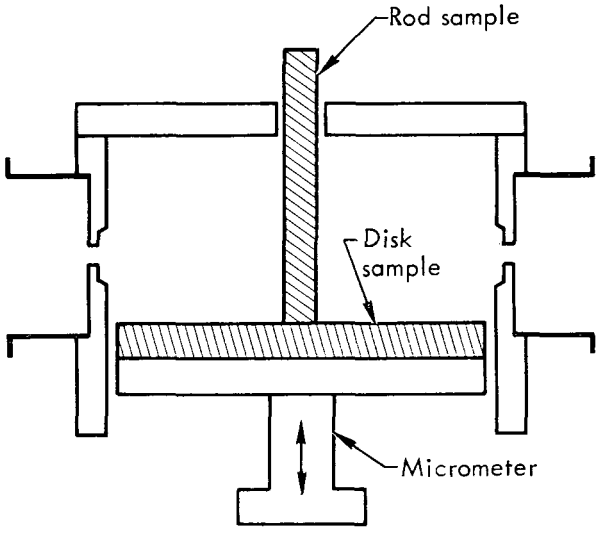

Fig. 3. Tunable TE_{oin} mode cavity resonator; either one of the two alternative sample forms is used.

evaluate the propagation constant in the sample (which is related to the complex dielectric constant of the sample). Electrode-sample contact problems can be overcome. Variations using open-circuit–short-circuit relations, resonant length measurements, and time domain reflection coefficient can also be used. (See Refs. 10, 14, 18, 27, 28.)

RESONANT CAVITY METHODS

A cavity resonator in the TE_{01} mode is convenient for dielectric measurements over an ϵ_r range of 1 to 100 or more and loss tangents from 10^{-5} to 1.0. Either disc or coaxial rod samples may be used (see Fig. 3). A difficulty is that any one cavity is rather narrow-banded. The analysis is based upon the impedance of the sample which is determined via the Q of the cavity, the dimensions of the cavity, and/or the cavity transmission coefficient.

A second cavity resonator method is a pertubation procedure using a rectangular waveguide resonator in a TE_{103} or TE_{105} mode. Observed data are the volumes of the cavity and the sample rod, and the resonant frequency and Q of the cavity with and without the sample. The real and imaginary parts of ϵ_r are known in terms of these quantities. (See Refs. 10, 29, 48.)

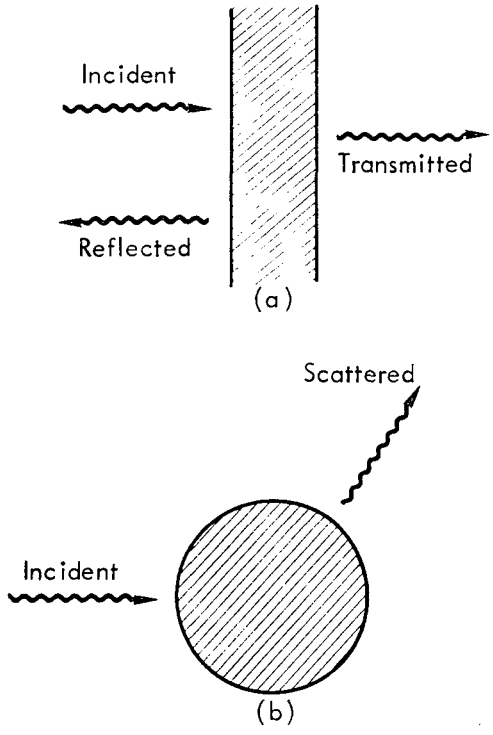

Fig. 4. Transmission and scattering techniques. (a) Planar sample; (b) spherical sample.

WAVEGUIDE METHODS

A slotted line measurement of the VSWR and phase of the standing wave with a slotted line waveguide terminated as in Fig. 2 enables one to compute the complex dielectric constant of the sample. (See Refs. 18, 23, 28.)

SCATTERING AND TRANSMISSION METHODS

The complex refractive index can be determined from comparisons of the theoretical solution and experimental results for scattering from a spherical sample and transmission through a planar sample (see Fig. 4). Extensive theoretical results are available for these situations. Very accurate phase and amplitude measurements are required. It is necessary that the sample be penetrable (i.e., the transmission loss through the sample should be measurable). Nonunique solutions are possible, but use of two different size samples can overcome this difficulty. (See Refs. 20, 24, 25.)

STANDARD SAMPLES AND COMPARISON MEASUREMENTS

A comparison of dielectric measurements[10] by the U.S.A., England and Canada over the range of 10^3 to 10^{10} Hz using standard samples and procedures has been made with accuracies of ±0.3%. Cavities were superior for measuring low losses. Standard samples of silica ($\epsilon_r = 3.82\text{-}j0.0005$) and glass ($\epsilon_r = 6.20\text{-}j0.033$) are available from the National Bureau of Standards.

In Situ Surface Measurements

FOUR-PROBE METHOD

Three common four-probe configurations are illustrated in Fig. 5. These configurations consist of two transmitter (current I) probes and two receiver probes. By using potential theory, one can determine the voltage difference V between the receiver probes for equal, but opposite direction, currents in the transmitter probes. The ratio of V to I depends only upon the geometric spacing (typically uniform as in Fig. 5) and the conductivity of the subsurface. Measurements are performed at a low enough frequency that induction effects and attenuation can be neglected. Contact resistance of the probes to the ground may be decreased by "watering" the ground around the probe and/or using many closely spaced probes in parallel. Receiver probes which are nonpolarizing electrodes are preferred. Insulated wires connecting the various probes are needed to decrease the cable pickup between the current (transmitter) wires and the voltage difference (receiver) wires. The Eltran array is more sensitive at small spacings, the Wenner array is more sensitive at large spacings, and the right angle array is somewhat between the Wenner and Eltran in sensitivity. The right-angle array has the advantage of the absence of mutual inductance between the transmitter and receiver circuits. (See Refs. 6, 12, 14, 16, 34, 43, 55, 63.)

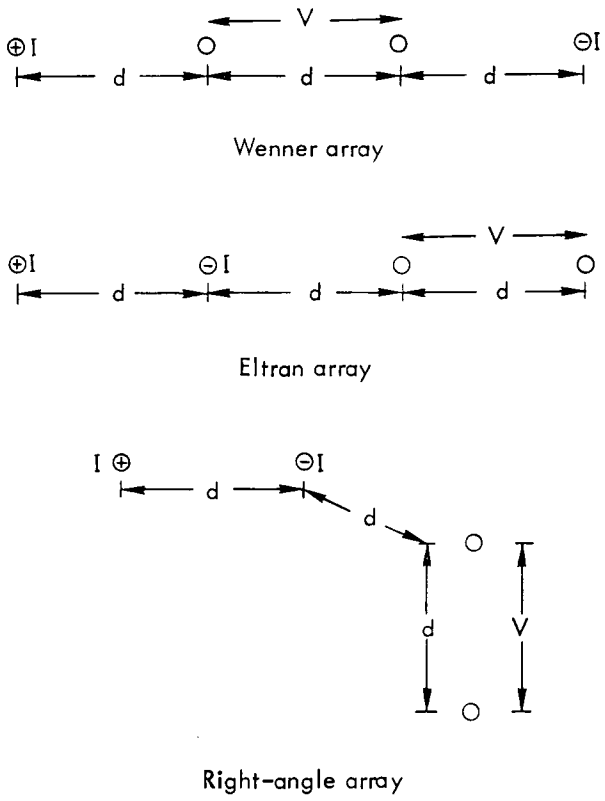

Fig. 5. Four-probe arrays.

TWO-LOOP METHOD

Measurement of the mutual impedance between two loops above ground enables one to estimate σ and ϵ_r of the ground. Four commonly used loop configurations are shown in Fig. 6.

Data interpretation curves (based upon Sommerfeld integrals) exist for homogeneous and vertically stratified grounds. Models include both conduction and displacement current effects. This mutual impedance procedure has been used for ELF to HF. This method has σ resolution problems when $\omega\epsilon_0\epsilon_r \gg \sigma$. (See Refs. 6, 14, 41, 42, 62.)

WAVE TILT METHOD

The tilt of an electromagnetic wave near the ground surface (see Fig. 7) at a

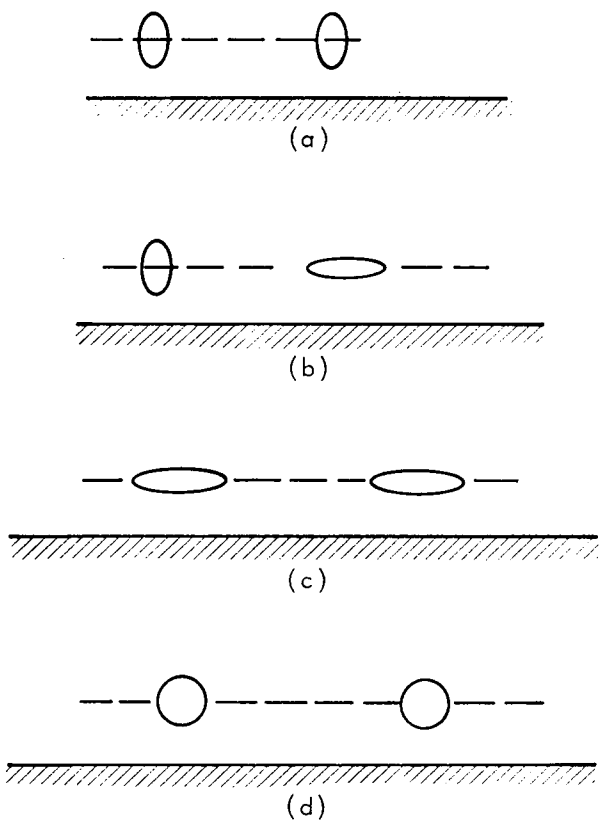

Fig. 6. Common loop configurations. (a) Coaxial; (b) perpendicular; (c) horizontal coplanar; and (d) vertical coplanar.

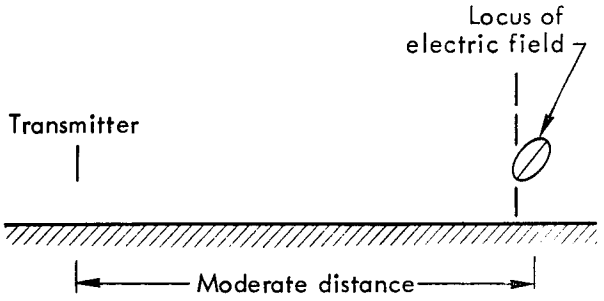

Fig. 7. Illustration of wave tilt.

moderate distance from the transmitter is simply related to the local ground conditions.

The electric field vector traces out an ellipse as a function of time at the observation point. By measuring the major and minor axes of the ellipse, or the radial and vertical fields, the wave tilt can be determined. If the local ground is homogeneous, this method works well when the ground is not too highly conducting or very lossless. Measurement accuracies then become acute, leading to possible uncertainties in either σ and/or ϵ_r. If the local ground is stratified many possibilities occur, some of which lead to erroneous results. This method has been used for frequencies of 100 kHz to 10 MHz for ground conditions of $\sigma = 10^{-4}$ to 10^{-2} mho/m and $\epsilon_r = 10$ to 40. (See Refs. 14, 16, 33, 39, 43, 46.)

POWER REFLECTIVITY

Determining the reflection coefficient at the ground surface enables one to estimate σ and ϵ_r of the ground (see Fig. 8). This method is also useful for a stratified medium with a low loss upper layer. Time of arrival measurements are helpful in determining the thickness

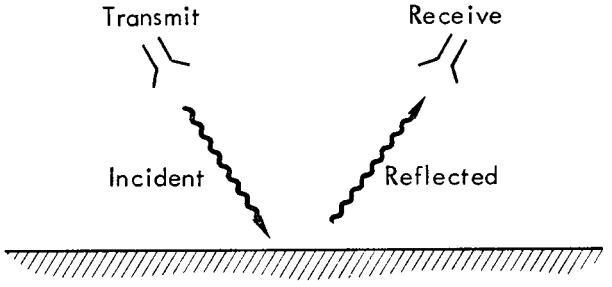

Fig. 8. Ground reflection.

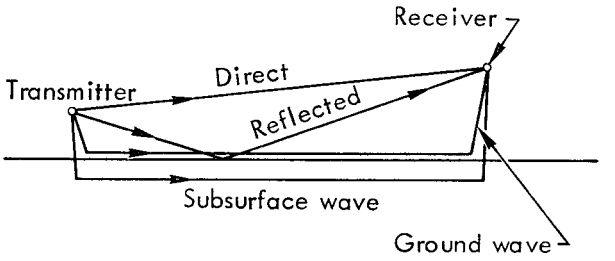

Fig. 9. Possible modes of propagation.

of the upper layer, and attenuation measurements are helpful in evaluating the conductivity of the upper layer. Surface roughness can invalidate this procedure. (See Refs. 14, 44, 45, 48.)

MULTIPLE MODE INTERFERENCE

For transmitter and receiver near the surface of the ground, a number of possible modes of propagation are feasible (see Fig. 9).

For large enough transmitter and receiver heights, and orientations such that the direct, groundwave, and subsurface wave are negligible, this situation reduces to the power reflectivity situation shown in Fig. 8. For transmitter and receiver near the surface, the direct and reflected waves effectively cancel each other and the ground wave and subsurface wave enables one to determine the σ and ϵ_r of the ground. The theory for this situation is founded upon the fundamental Sommerfeld integrals. More approximate procedures (ray optics) are sufficient in some cases. Mode interference also occurs for a stratified ground and for buried transmitter and receiver. (See Refs. 14, 47.)

ANTENNA INPUT IMPEDANCE METHODS

The input impedance of an antenna close to the earth (see Fig. 10) is dependent upon the electric parameters of the ground. Horizontal linear antennas near resonant length and within one-tenth wavelength of the ground have been shown to be effective for determining σ and ϵ_r of the ground. Antennas lying on the surface are quite effective as they are closely coupled to the earth. Vertical antennas are not as effective as horizontal ones (for this purpose) as they do not couple as strongly to the earth. An apparent "shortening" of the physical length for an antenna lying on the surface is evident in the impedance variation relative to its behavior in free space. Surface roughness, stratification, and local anomalies can mask the actual subsurface structure. It is advisable to perform measurements at several different frequencies or antenna lengths. (See Refs. 14, 32, 48, 67.)

FIELD VARIATION WITH DISTANCE METHODS

The theoretical dependence of field strength upon distance from the transmitter (see Fig. 11) is expressed in terms of the conductivity σ and relative dielectric constant ϵ_r of the ground. Hence, for a reasonably homogeneous ground, knowledge of the field strength behavior with distance enables one to estimate the local σ and ϵ_r. Theoretical results now exist not only for a uniform flat earth, but for certain inhomogeneous composition, spatially-varying terrains. A notable example of the application of this technique is the effective conductivity map of the United States, estimated by observing the field decay with distance of U.S. commercial radio stations. (See Refs. 6, 14, 16, 30, 31, 35, 36, 37, 38, 40, 47.)

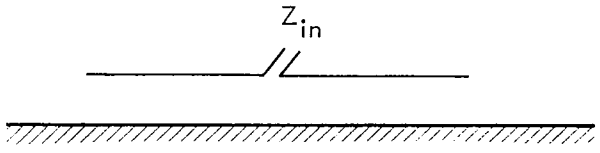

Fig. 10. Input impedance.

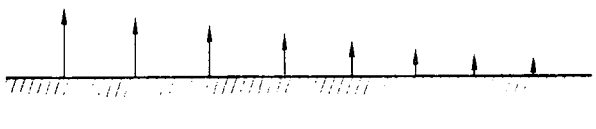

Fig. 11. Field variation with distance.

In Situ Drill Hole Measurements

TWO-LOOP METHODS

The mutual impedance of two loops in an infinite uniform medium is dependent upon the relative orientations, the separation distance, and the medium electrical parameters. Theoretical results for the mutual impedance dependence of coaxial and coplanar loops upon ϵ_r and σ exist.

It has further been shown that under most conditions, the mutual impedance of coaxial loops in a drill hole (see Fig. 12) does not depend upon the presence of the drill hole. Measurements of Z_{mutual} of two coaxial loops in a drill hole, to determine ϵ_r and σ, have been successfully correlated with alternative ground-parameter measurement schemes. This method is a simple and accurate means of probing the electrical parameters of the medium immediately surrounding the drill hole. (See Refs. 59, 60, 63.)

SURFACE-TO-HOLE METHODS

For a transmitter in a drill hole and a receiver on the surface (see Fig. 13), the field attenuation and phase shift between transmitter and receiver are related to the σ and ϵ_r of the ground.

Knowledge of the geometry of the situation, the patterns and impedances of the transmitter and receiver, and the input power level enables one to use propagation models to estimate σ and ϵ_r for the medium through which the signal passed. Subsurface anomalies, particularly near the surface, can have a decided effect upon the data quality. (See Refs. 15, 55, 63.)

ANTENNA INPUT IMPEDANCE METHODS

Wire radiators may be used to deduce the electrical properties of the medium from the measured input impedance (see Fig. 14). A variety of linear antenna

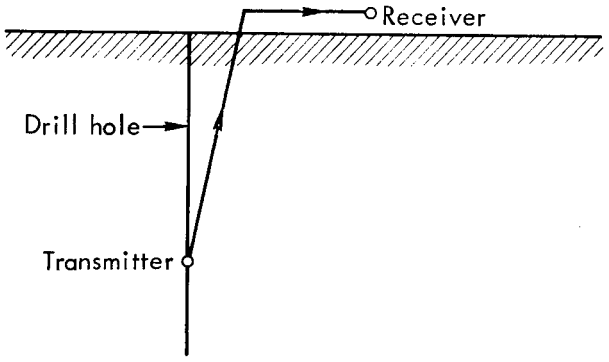

Fig. 13. Surface-to-hole situation.

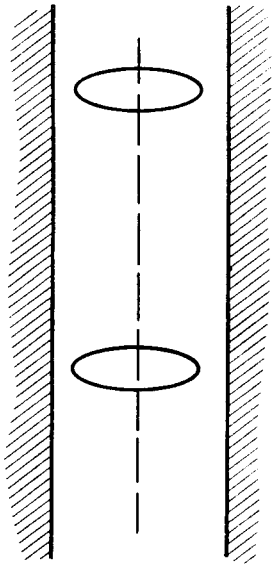

Fig. 12. Coaxial loops downhole.

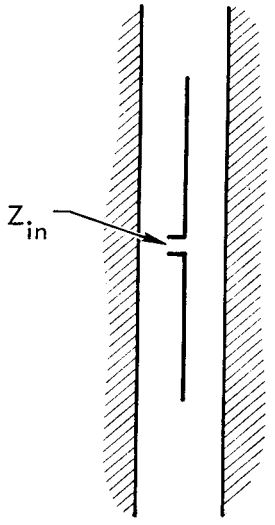

Fig. 14. Antenna input impedance.

types have been used: electrically long insulated antennae, near resonant length antennae, and electrically short probes. These methods are accurate for evaluating σ (when $\sigma >> \omega\epsilon_0\epsilon_r$) or ϵ_r (when $\omega\epsilon_0\epsilon_r >> \sigma$). They are useful for determining the electrical parameters of the medium within one skin depth of the drill hole. (See Refs. 16, 54, 56, 61, 63.)

AXIAL ELECTRIC FIELD DECAY METHOD

This method (see Fig. 15) is based upon the axial field decay of the field in the rock medium between separated transmitter and receiver. The exponential decay of the signal with skin depth enables one to determine the skin depth, and from this σ (assuming ϵ_r is known). An encapsulated transmitter is preferred to reduce cable pickup difficulties. This technique is useful for probing the medium within one skin depth of the drill hole. (See Refs. 16, 51, 63.)

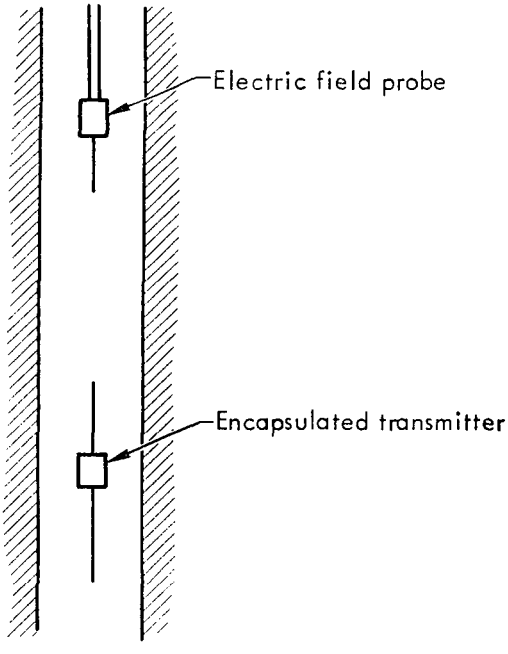

Fig. 15. Axial electric field variation.

TRANSMISSION LINE METHOD

Unshielded balanced parallel wire transmission lines inserted into a drill hole may be used to deduce the σ and ϵ_r of the ground. Standard open-circuit–short-circuit procedures may be used to determine the characteristic impedance and propagation constant of the transmission line. These quantities may then be used to estimate σ and ϵ_r. (See Refs. 14, 16, 49.)

HOLE-TO-HOLE TRANSMISSION METHODS

For a transmitter in one drill hole and a receiver in a second drill hole (see Fig. 16), or a second receiver in a third drill hole (see Fig. 17), there are a variety of methods of determining σ and ϵ_r of the intervening medium.

For the situation shown in Fig. 16, measurement of the absolute attenuation and phase shift (for cw signals) or the time of arrival (for pulse signals) enables one to evaluate σ and ϵ_r of the sub-surface. Hole separations greater than a wavelength have yielded reliable data. Alternate modes of propagation (e.g., up-over-down and surface-reflected) rather than the

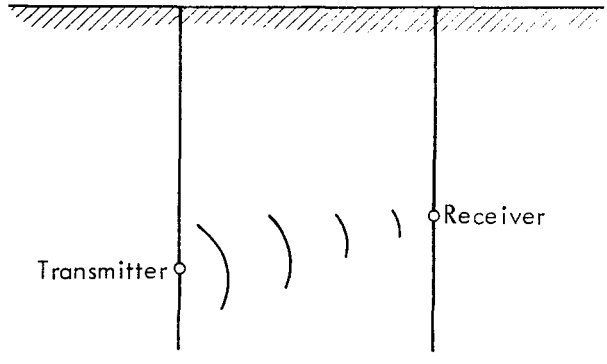

Fig. 16. Two-hole method.

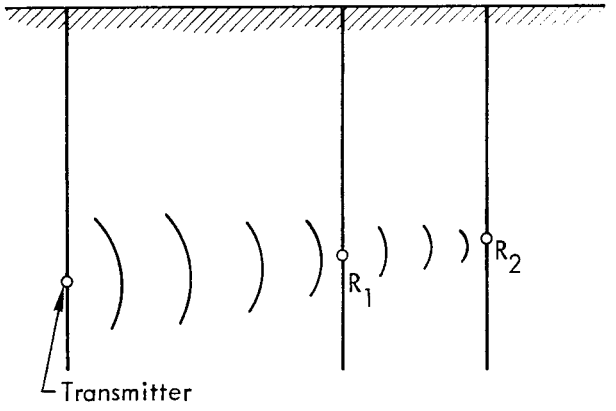

Fig. 17. Three-hole method.

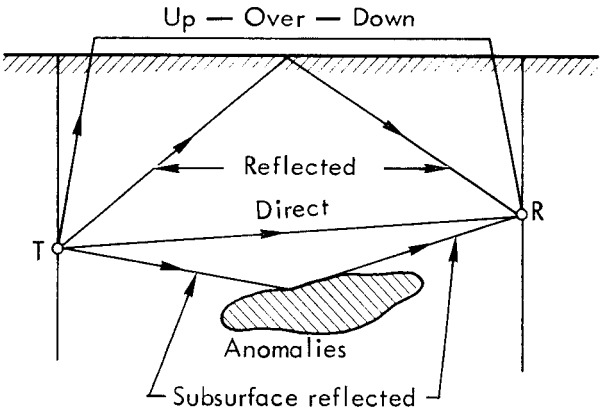

Fig. 18. Interference modes.

direct mode can contaminate the data; however, these interference phenomena can also be used to determine the medium properties (see next section). This method is not useful in media with hole separations of many skin depths. For the situation shown in Fig. 17, the differential phase shift and differential attenuation between receivers R_1 and R_2 enables one to estimate σ and ϵ_r. The measurement accuracies are not as severe for the three-hole situation as for the two-hole situation; however, the extra expense of the third hole may not be justified. (See Refs. 16, 52, 53, 55, 56, 57, 58, 62, 63.)

INTERFERENCE PHENOMENA METHODS

For the situation shown in Fig. 18, there are a number of possible modes of propagation (direct, reflected, up-over-down, subsurface reflected) any one of which may be dominant (dependent upon a number of factors). Depending upon the relative level of the different modes, various interference phenomena are feasible. If only two modes are competitive (e.g., the direct and reflected), then ray optic procedures may be used with the differential path differences to predict the notching (in-phase and out-of-phase) behavior of the received signal with frequency variation. For pulse excitation, time of arrival may be used to separate the various modes and their attenuation. (See Refs. 52, 62, 63.)

FOUR-PROBE METHODS

The four-probe method is applicable in drill holes as well as on the surface. Potential theory can be used to determine the mutual impedance between transmitter (current) and receiver (voltage difference) probes. This mutual impedance depends only upon geometric factors and the ground conductivity. A number of variations of transmitter and receiver probe locations have been used. (See Refs. 14, 62, 63.)

Model Measurements

In various cases, experimental data for validating theoretical calculations (and the associated measurement scheme) or experimental data for testing the

feasibility of a measurement scheme is difficult to obtain for a number of controlled situations.[14,64-68] For example, varying the in situ water content, the salt content, the tide level, the geologic constituents, and the geometric locations of transmitter and receiver may be exceedingly difficult, time-consuming, and expensive to perform with full-scale in situ measurements. In addition it may be difficult, time-consuming and expensive to obtain numerical results for a theoretical model of the physical situation. When these situations occur, it is sometimes useful to perform scale-model experiments. This can be a difficult task for a homogeneous medium, and even more difficult for an inhomogeneous medium. Nevertheless, models for complicated media have been constructed and have led to useful results. This method has had extensive use in determining the effect of subsurface anomalies on surface measurement schemes.

Sample Results for σ and ϵ_r

Numerous results have been obtained[1,4,6-8,11,12,14,19,22,26,28,33,45,47,55-57,62,63] for σ and ϵ_r of earth materials under a variety of conditions. Factors which have a decided influence upon σ and ϵ_r are the frequency, the water content, geological constituents, temperature, weathering factors, and local anomalies, among others. "Nominal" results for commonly encountered media can be

Table 1. Nominal terrain constants (from Ref. 11).

	> 3 m		10 cm		3 cm		1 cm	
Wavelength	ϵ_r with respect to vacuum	σ^a (mho/m)	ϵ_r	σ	ϵ_r	σ	ϵ_r	σ
Sea water	80	1-5	69	6.5	65	16	22	50
Fresh water	80	0.001-0.1						
Humid soil, clay	30	0.01-0.02	24	0.6				
Fertile cultivated soil	15	0.005						
Grass, meadow, race courses, sports grounds			3-6	0.05 -0.11				
Rocky ground	7	0.001						
Urban areas, large towns	5	0.001						
Dry soil	4	0.01						
Very dry soil, deserts	4	0.001-0.0001	2	0.03	about 3	0.007 -0.1		

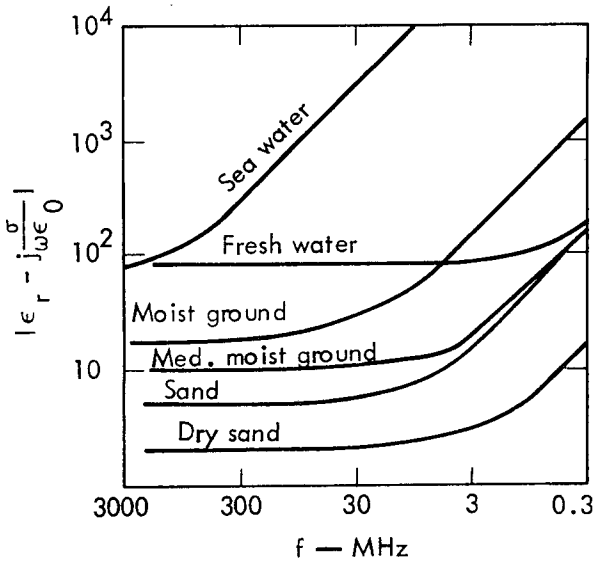

Fig. 19. ϵ_r dependence upon frequency and terrain type.

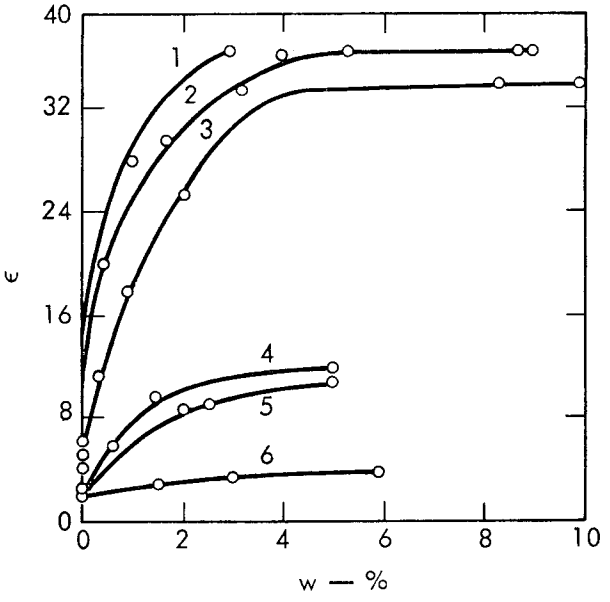

Fig. 20. ϵ_r dependence upon the water content percentage (from Ref. 7).

looked up in tables; however, these numbers should be used with discretion. Due to the variability of σ and ϵ_r from site to site and with environmental factors, it is prudent to determine ϵ_r and σ for a particular site rather than rely on "textbook" values.

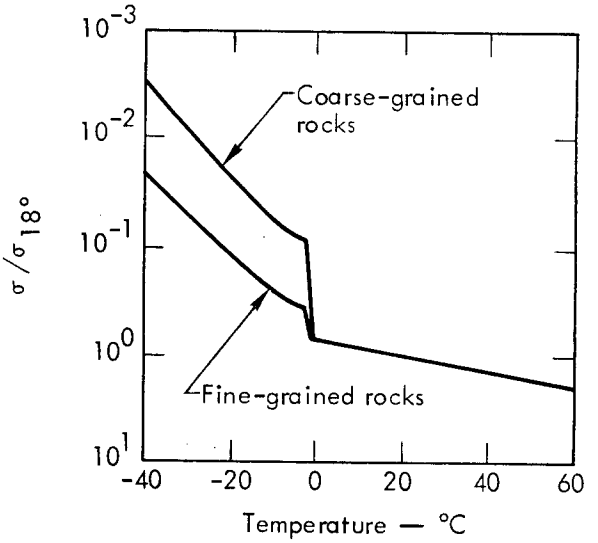

Fig. 21. Change in conductivity of rocks as they pass through the freezing point (from Ref. 14).

Three of the factors which have the most effect upon σ and ϵ_r are the geologic constituents, the water content, and the frequency. A representative dependence of various earth media ϵ_r and σ values is given in Table 1.[11] Note that as the frequency increases, typically ϵ_r decreases and σ increases.

Media with a high water content have a higher dielectric constant and conductivity than those with less water. This is seen[8] in Fig. 19 which depicts nominal results for $|\epsilon_r - j\sigma/\omega\epsilon_0|$.

An explicit dependence of ϵ_r upon the water content[7] of rocks is shown in Fig. 20. The dielectric constant behavior[4] of sample earth medium with frequency is given in Table 2. Note the dramatic temperature difference of ϵ_r for water and ice. A similar variation[14] occurs for rocks (see Fig. 21). Survey maps of the conductivity of large areas have been performed at high frequencies[6] and at low frequencies.[12] Examples of these maps are given in Fig. 22 (for high

Table 2. Behavior of sample earth medium.

Material	Composition	Temp. (°C)	ϵ_r at frequency (Hz)			
			10^3	10^6	10^8	10^9
Soil	Sandy dry	25	2.91	2.59	2.55	2.55
Soil	Loamy dry	25	2.83	2.53	2.48	2.44
Ice	From pure distilled water	-12		4.15	3.45	3.20
Snow	Freshly fallen	-20	3.33	1.20	1.20	1.20
Snow	Hard-packed followed by rain	-6		1.55		1.5
Water	Distilled	25		78.2	78	76.7

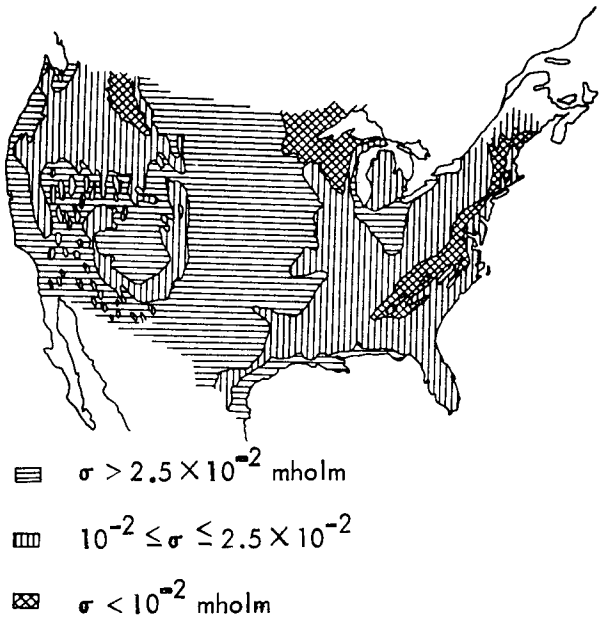

Fig. 22. Ground conductivity map of the United States based on a correlation between resistivities determined from the decay of radio-station fieldstrengths and geological sub-outcrop (Keller and Frischknecht, 1966).

frequencies) and in Fig. 23 (for low frequencies).

Nominal values of various ground media are given in Table 3 for ϵ_r, and in Table 4 for resistivity $\rho = 1/\sigma$.

There is a great deal of interest in the electrical properties of resources (such as coal and oil). Numerous measurements have been performed on coal, and the resistivity (or conductivity) results cover a wide range. The main factor in determining the resistivity of a coal[7] is the

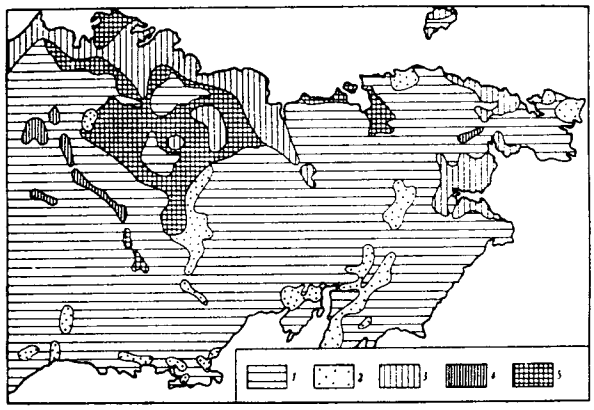

Fig. 23. Schematic map of the electric conductivity of the frozen rocks in the Northeastern USSR: (1) Frozen rocks with an electric conductivity greater than $1.67 \cdot 10^{-4}$ mho/m; (2) frozen rocks with an electric conductivity ranging from $1.67 \cdot 10^{-4}$ to $4 \cdot 10^{-5}$ mho/m; (3) frozen rocks with an electric conductivity ranging from $4 \cdot 10^{-5}$ to 10^{-5} mho/m; (4) frozen rocks with an electric conductivity ranging from 10^{-5} to $2.5 \cdot 10^{-6}$ mho/m; (5) frozen rocks with an electric conductivity of less than $2.5 \cdot 10^{-6}$ mho/m.

Table 3. Dielectric constants of rocks.

Rock	Source, mineral composition (%)	ϵ_r	Frequency (Hz)	Water content (%)
Sedimentary rocks				
Anhydrite with gypsum	anhydrite, 92 gypsum, 8	6.3		dry
"Chuneski" shale, bentonitic		10-45.0	10^2-10^6	10
The same		4-7.0	10^2-10^6	dry
"Gumbrin" shale, bentonitic		9.5-10	10^2-10^6	dry
Dolomite		8.0-8.6	10^3-10^7	dry
Limestone	Georgian SSR	7.3		dry
Limestone		8.0-12.0		–
Arkosic sandstone	quartz, 23 feldspar, 75 mica, 2	4.9		dry
Quartz-feldspar sandstone	quartz, 40 feldspar, 45 other, 15	5.1		dry
Sandstone	Garm	4.66	5×10^5	dry
	Zubovskoe	3.96	5×10^5	dry
Variegated sandstone		9.0-11.0		
Shaly sandstone		5.53		dry
The same		7.17		0.2
Metamorphic Rocks				
Amphibolite		7.9-8.9	10^5-10^7	dry
Gneiss		8.0-15.0		
Granite gneiss		8.0-9.0	5×10^2-5×10^7	
Quartzite	Shokshinskoe	4.36	5×10^5	dry
Quartzite	Ridderskoe	4.85	5×10^5	dry
Quartzite		6.6		
Quartzite		7.0		
Marble		8.22		dry
Marble		8.37		0.002
Marble		8.9-9.0	10^3-10^7	dry
Talc slate		7.5-34.0	5×10-5×10^7	dry
Micaceous slate		9.0-10.0	5×10-5×10^7	dry
Roofing slate	Georgian SSR	6.71		dry
Roofing slate	Georgian SSR	7.74		0.1
Phyllite		13.0		
Igneous rocks, acid				
Biotite-granite aplite	quartz, 40 microcline, 32 plagioclase, 20 other, 8	4.8		dry
Granite	Altai	5.42	5×10^5	dry
Granite	Leznikovskoe	4.74	5×10^5	dry

Table 3. (Continued)

Rock	Source, mineral composition (%)	ϵ_r	Frequency (Hz)	Water content (%)
Granite	Garm	5.06	5×10^5	dry
Granite	Valaamskoe	4.5	5×10^5	dry
Granite		7.0-9.0		combined moisture
Volcanic tuff		3.8-4.5		dry
Igneous rocks, intermediate				
Diorite	Kola Peninsula	5.9-6.3	10^5-10^7	dry
Diorite		8.5-11.5	10^4-10^7	dry
Dacite		6.8-8.16	3×10^6	
Igneous rocks, basic				
Augite porphyry	Kola Peninsula	9.5-12.6	10^5-10^7	dry
Basalt	Berestovetskoe	15.6	5×10^5	dry
Basalt	Kutai	10.3	5×10^5	dry
Gabbro		8.8-10.0	10^4-10^7	dry
Gabbro	Southern Urals (3.26% ore content)	12.8		dry
Diabase	Oneshsk	11.6	5×10^5	dry
Diabase		9.0-13	10^4-10^7	dry
Labradorite	Ukrainian SSR	7.82		
		8.24		0.03
Igneous rocks, ultrabasic				
Peridotite (Plagioclase)	Kola Peninsula	15.7-18.8	10^5-10^7	dry
Peridotite		12.1	5×10^5	dry
	olivene 70 augite, 25 mica, 5	8.6		dry
Olivene pyroxenite	Kola Peninsula	8.4-9.5	10^5-10^7	dry
Igneous rocks, alkaline				
Syenite		6.83	5×10^5	dry
Syenite		13.0-14.0		dry
Aegerine-phyllite nepheline syenite	Kola Peninsula	6.93		dry
Mica nepheline syenite with aegerine	Kola Peninsula	8.47		dry
Microcrystalline nepheline syenite	Kola Peninsula	9.55		dry
Aegerine nepheline syenite		9.56		dry
Fayalite	near Mariupol	8.32		dry
Luyavrite	Kola Peninsula	9.7-11.4	10^5-10^7	dry
Urtite	Kola Peninsula	7.3-8.5	10^5-10^7	dry
Felspathic urtite	Kooshva	11.9		dry

Table 4. Resistivities of rocks.

Rock type	Source	Resistivity (ohm.cm) Wet	Dry	Comments
Sedimentary rocks				
Dolomite	Armenian SSR	3.5×10^4-5.0×10^5		
Limestone	Kazakhstan SSR	4.2×10^7	1.2×10^9	Dolomitized form
Limestone	Georgian SSR	2.1×10^7	2.3×10^9	
Limestone marl	Georgian SSR	8.4×10^8		Fine-grained rocks
Sandstone	Donbas	1.41×10^7	6.4×10^{10}	Water content, 0.37%
Sandstone	Kara-Shishak	3.5×10^6	3.1×10^7	
Arkosic sandstone	Jezkazgan	6.8×10^4	1.0×10^8	
Quartzitic sandstone	Dashkesan	2.3×10^4-3.3×10^4		
Tuffaceous sandstone	Dashkesan	10^5-1.0×10^7		
Metamorphic rocks				
clay slate	Georgian SSR	6.4×10^6	1.6×10^7	Strongly quartzitic
clay slate	Georgian SSR	1.1×10^6	1.6×10^9	
clay slate	Nerchinsk	1.0×10^5	1.0×10^8	
clay slate	Georgian SSR	4.0×10^5	6.0×10^8	Shaly
Quartz-sericite slate	Ziryanskii mine	5.0×10^6	3.6×10^9	
Quartz-chlorite slate		5.0×10^5	2.0×10^8	
Calcareous quartzite	Altai	4.0×10^5	2.0×10^{10}	
Quartzite	Georgian SSR	4.7×10^8		
Metamorphosed tuff	Altai	2.0×10^5	1.0×10^7	
Gneiss	Kugrasin	6.8×10^6	3.2×10^8	
Marble	Nerchinsk	1.4×10^6	2.5×10^{10}	
Marble		7.06×10^{11}	1.8×10^{20}	
Hornfels	Kugrasin	6.0×10^7	6.0×10^8	
Hornfels	Trans-Caucasus	8.1×10^5	6.0×10^9	
Skarn	Armenian SSR	2.5×10^4		
Igneous rocks, Acidic				
Granite	Azerbaidjan SSR	3.0×10^7		
Granite	Ubinskoe	0.36×10^9	3.2×10^{18}	
Granite	Kola Peninsula	0.16×10^9	0.3×10^{16}	
Granite porphyry		4.5×10^5	1.3×10^8	
Granite porphyry	Urals	7.0×10^5	1.0×10^7	
Quartz vein	Komsomol'skoe	0.6×10^{10}	1.0×10^{18}	
Quartz porphyry	Georgian SSR	9.2×10^7		
Feldspar porphyry	Australia	4×10^5		
Leucophyre (albite)	Georgian SSR	2.9×10^4	0.4×10^9	

Table 4. (Continued)

Rock type	Source	Resistivity (ohm · cm) Wet	Dry	Comments
Leucophyre (albite)	Urals	4.5×10^5		
Intermediate				
Porphyrite	Georgian SSR	10^3	3.3×10^5	
Porphyrite	Azerbaidjan SSR	6.7×10^4		
Porphyrite	Dashkesan	5×10^6		
Diorite porphyry	Caucasus	1.9×10^5	2.8×10^6	
Carbonitized porphyry	Armenian SSR	2.5×10^5	5.9×10^6	
Diorite	Urals	2.8×10^6		
Quartz diorite	Azerbaidjan SSR	2.0×10^6	1.8×10^7	
Quartz diorite	Georgian SSR	2.0×10^8		
Dacite	Georgian SSR	2.1×10^6		
Andesite	Georgian SSR	4.5×10^6	1.7×10^4	
Basic and ultrabasic				
Diabase porphyry	Trans-Caucasus	9.6×10^4	1.7×10^7	
Diabase	Karelaia	3.0×10^6	2.2×10^{11}	
Diabase	Georgian SSR	3.8×10^4	3.3×10^7	
Diabase	Georgian SSR	2.9×10^4	0.8×10^9	
Diabase	Sibaevskoe	4.57×10^9		
Diabase	Blyavinskoe	1.18×10^7	1.0×10^{12}	
Diabase	Khibini	0.16×10^8	0.17×10^{13}	
Olivine norite		3×10^6-6×10^6		
Olivine norite		10^5-6×10^5		
Basalt	Armenian SSR	1.6×10^5		
Basalt	Berestovetskoe	2.3×10^6	1.3×10^9	
Peridotite		3.0×10^5	6.5×10^5	

degree of metamorphism which causes differences in carbonization and carbon ratio. Coals have been widely classified according to the degree of carbonization as follows:

1. Brown coal (B)
2. Long-burning coal (D)
3. Gassing coal (G)
4. Greasy steam coal (bituminous) (PSh)
5. Coking coal (K)
6. Lumpy steam coal (superbituminous) (PS)
7. Lean coal (subanthracite) (T)
8. Anthracite (A)

The carbon ratio and the ash content both increase in going from the top to the bottom of this list. Figure 24 depicts measured values of resistivity for the various types of coal.

A complicating factor which can influence results of resistivity measurements is that the resistivity parallel to the bedding plane may not be equal to the resistivity normal to the bedding plane. The resistivity parallel to the bedding plane (ρ_P) is normally less than the resistivity normal to the bedding plane (ρ_N). This dependence of resistivity upon direction is an anisotropy

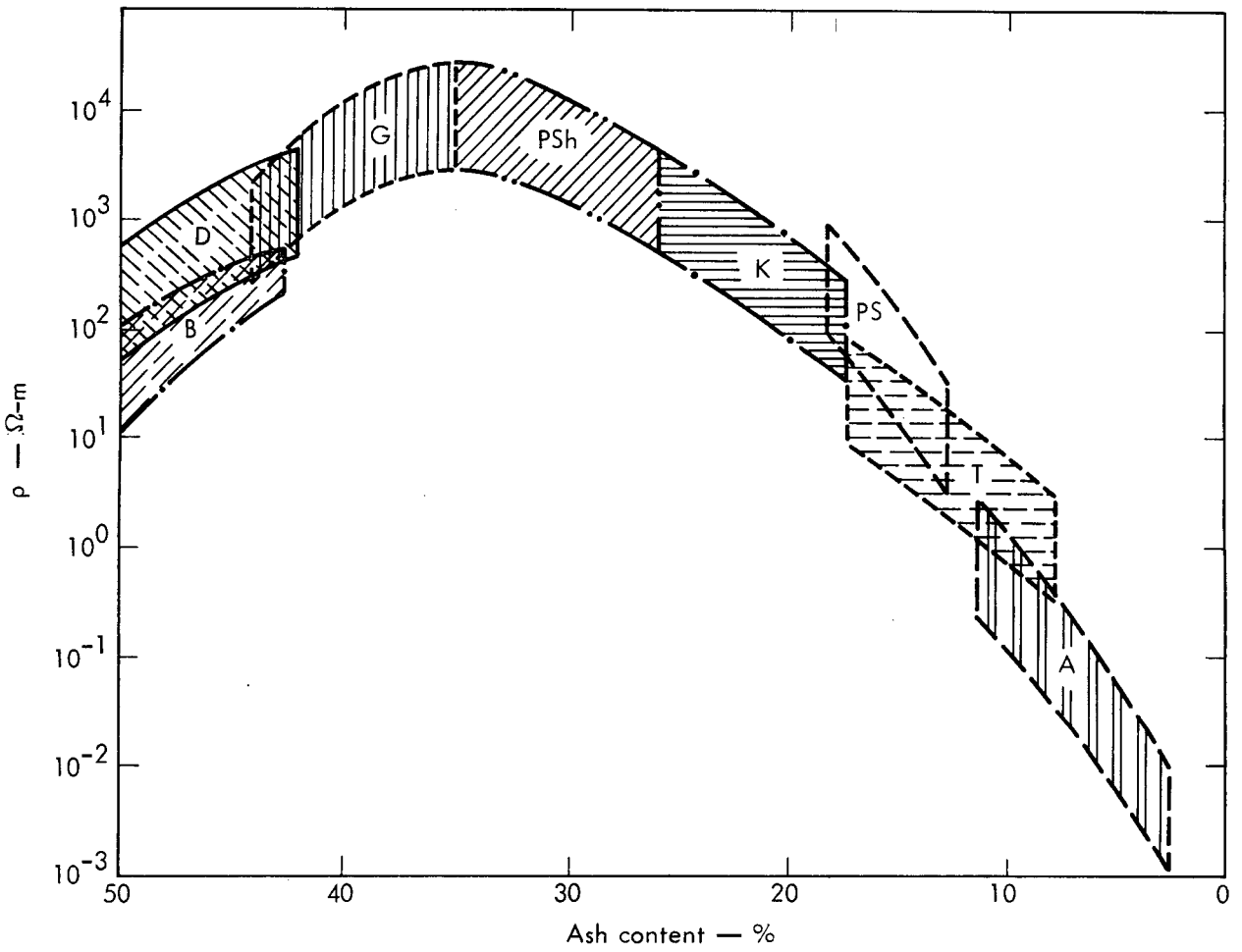

Fig. 24. Graph of the most probable values for the resistivity of coals of various grades as a function of quality. The ash content is plotted along the abscissa. (From Ref. 7.)

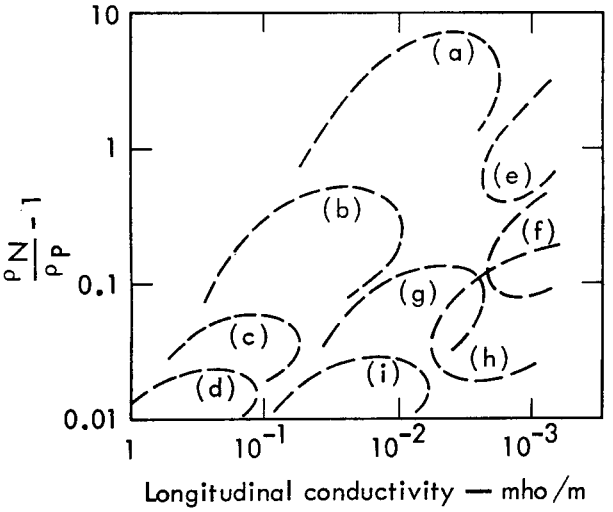

Fig. 25. Summary of common ranges for values for the coefficient of macroanisotropy and longitudinal conductivity for thick sequences of rock. (a) Evaporites, (b) limestone, (c) sandstone, (d) shale, (e) slate, (f) gabbro, (g) volcanics, (h) granite, and (i) alluvium. (From Ref. 7.)

in the medium. A measure of the degree of anisotropy is the ratio of ρ_N to ρ_P. Sample results for ρ_N/ρ_P for a variety of rock types is shown in Fig. 25. The degree of anisotropy is not large except for slate and evaporites.

The permeability μ of earth medium is usually that of free space, or $\mu = \mu_0 = 4\pi\ 10^{-7}$. However, when there is a significant magnetite content in the rock,[6] the permeability increases (see Fig. 26).

For more details about the dependence of σ, ϵ_r, and μ upon these and other factors, the reader is referred to the various references and the literature.

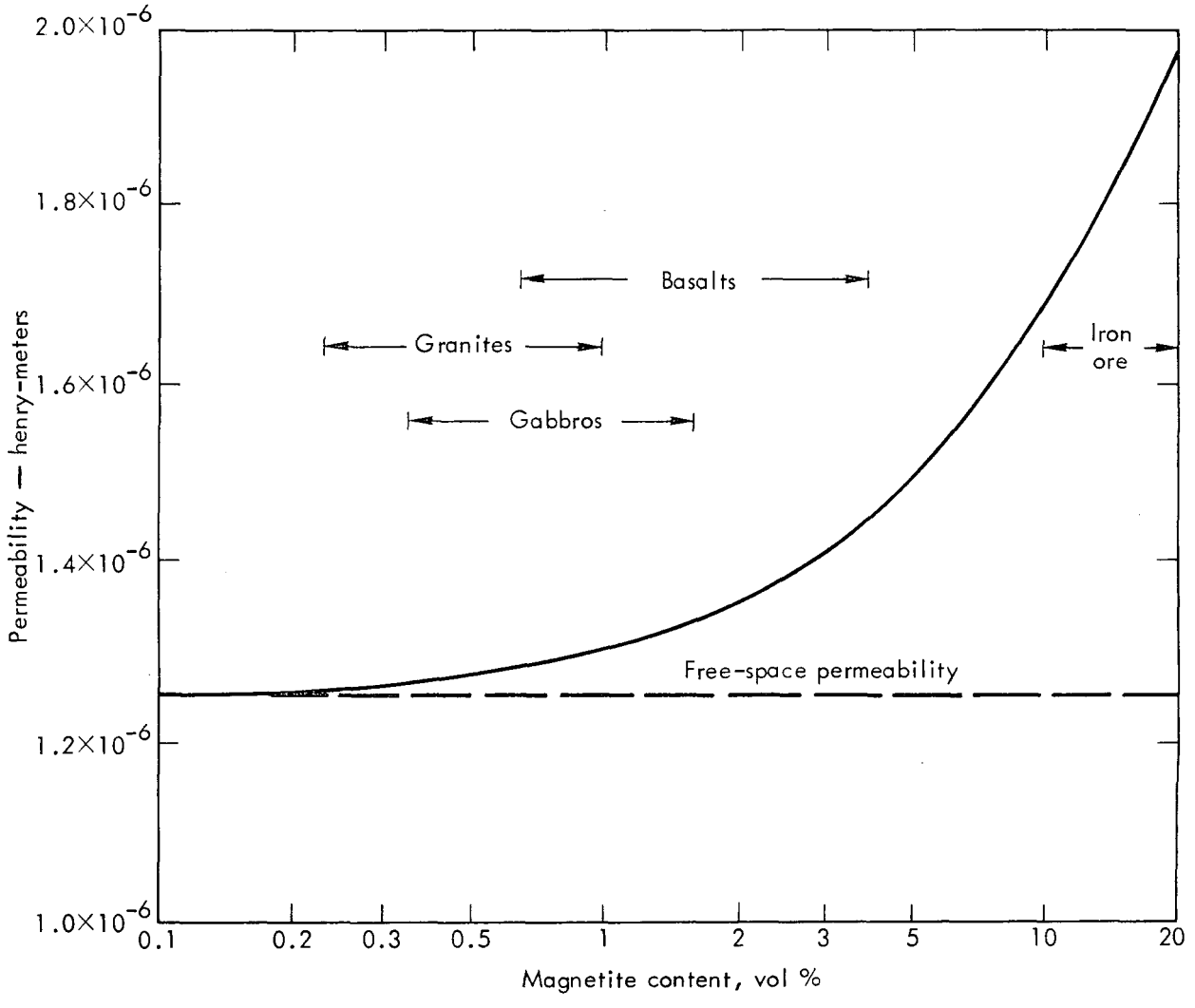

Fig. 26. Observed relationship between the amount of magnetite in a rock and magnetic permeability. (From Ref. 6.)

Application to Geophysical Probing and Profile Determination

The problem of determining the subsurface profile of a medium (by measurements performed on the surface and/or in drill holes) can be designated as the

inverse scattering or inverse transmission problem. The mathematics used to solve electromagnetic ground parameter profile problems also arise and have been used in a number of other physical situations. For example, ground-based and satellite-borne remote probing systems are used in atmospheric physics probing techniques based on inverse scattering and inverse transmission data reduction methods.

Measurement methods which have been applied to determining subsurface electrical parameter profiles include four-probe (for mineral exploration, location of salt domes, identification of gravel deposits or mineral nodules on the ocean floor), two-loop mutual impedance (for detection of buried objects, determining the depth of permafrost), wave tilt (for defining gravel deposits), and multiple-mode interference phenomena (for determining depth of the water table, the electrical parameters near the surface of the moon, locating subsurface anomalies surrounding a drill

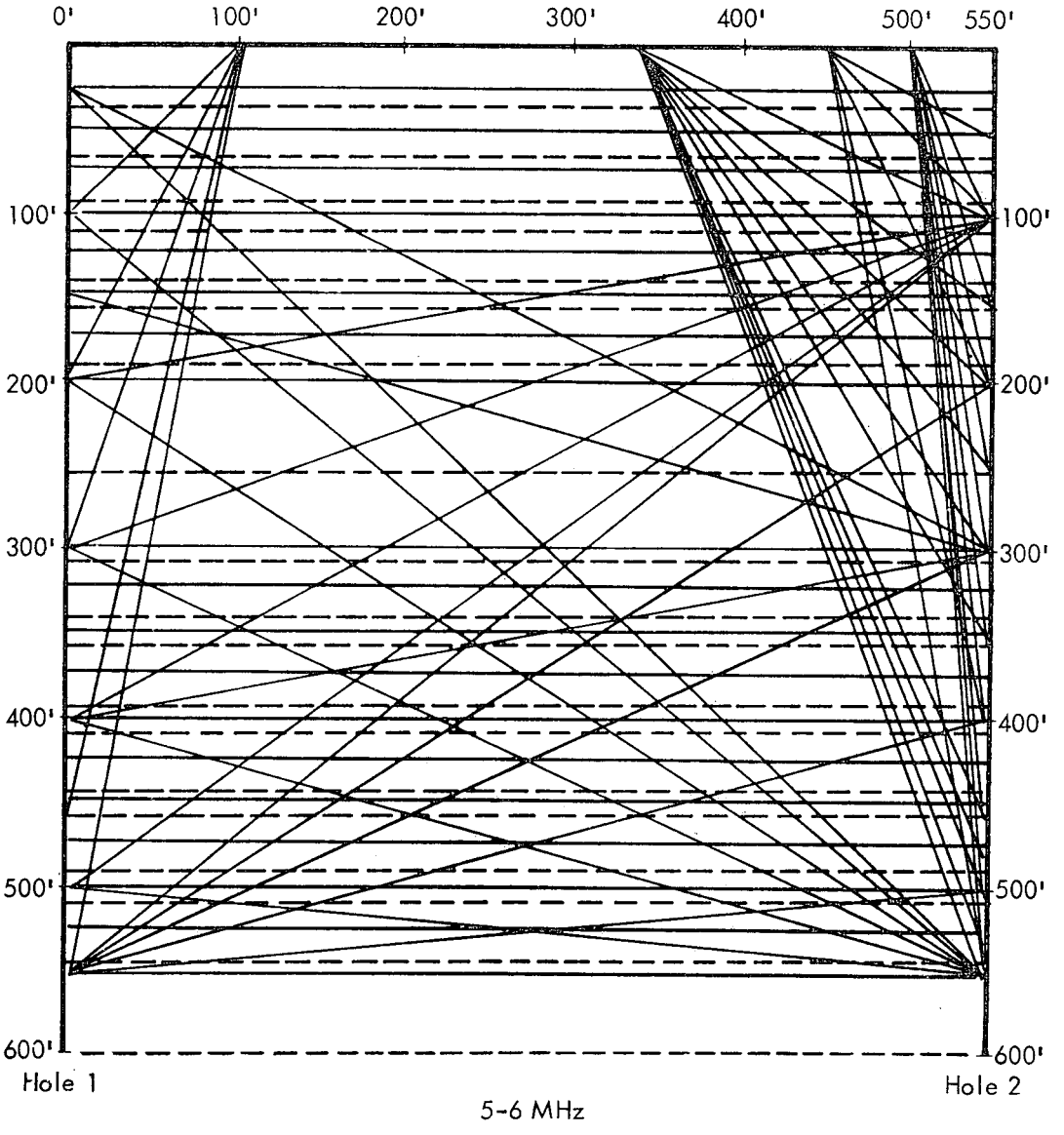

Fig. 27. Experimental setup.

hole, for determining glacial thickness, among others.)

Much consideration has gone into data reduction procedures to be used to invert the "inverse data." Procedures which have been successful include least-square matrix methods, parameter optimization techniques, iterative approaches, and perturbation methods.

An example of the inverse transmission problem using the drill hole surface-to-hole and hole-to-hole measurement methods is discussed below to illustrate results for the electrical parameter profile of a particular earth medium (hard rock in a permafrost zone in the Brooks Range in Alaska.[63] These results not only indicate what can be achieved in subsurface profile determination, but also indicate the frequency dependence of ϵ and σ and the variation of ϵ and σ with temperature and water content. Additional data were also taken at the site showing how multiple-mode interference phenomena can be used to detect anomalies in ground parameters.

Figure 27 depicts the experimental situation for a frequency sweep of 5-6 MHz. There are two drill holes, each of the order of 600 ft deep, with a separation distance between holes of 550 ft. The solid lines in Fig. 27 indicate direct-ray paths between transmitter and receiver (note that hole-to-hole and surface-to-hole paths are shown). The dotted lines in Fig. 27 are an assumed subsurface ϵ_r dependence upon depth (to be determined). By monitoring the phase shift between transmitter and receiver, ϵ_r was determined for the frequency ranges of 5-6, 12-13, and 20-21 MHz.

The variation of ϵ_r with depth and frequency is illustrated in Fig. 28. Note that as the frequency increases, ϵ_r normally decreases (as expected). There seems to be an anomalous behavior near 425 ft. This was found to be the bottom of the permafrost, hence the water in the rock was frozen above 425 ft and not frozen below 425 ft (leading to an increase in ϵ_r). The decrease in ϵ_r at the greater depths is possibly caused by the grain size of the rocks being finer at these depths, and hence the rock perhaps had a smaller water content.

Power loss measurements between transmitter and receiver provided a means of evaluating σ versus depth in a manner similar to that used for ϵ_r versus depth. Data results for σ versus depth are shown in Fig. 29. Note that σ typically increases as the frequency is increased, the conductivity increases near the bottom of the permafrost (perhaps due to the temperature change effect upon the water in the rock), and the conductivity decreases at the greater depths (perhaps due to a decrease in the water content in the rock).

Multiple-mode interference phenomena were used to show how a discontinuity in electrical parameters could be located via hole-to-hole transmissions. A strong electrical parameter discontinuity occurs at the ground-air interface. Its presence, and location relative to transmitter and receiver, can be determined by observing the interference of the direct and ground-air interface reflected modes (see Fig. 30). Due to the additional path length of the reflected ray relative to the direct ray, at some frequencies the direct and reflected ray path lengths will be in phase, and at other frequencies they will be out of phase. The frequency width between in-phase (or out of phase) points is dependent upon the

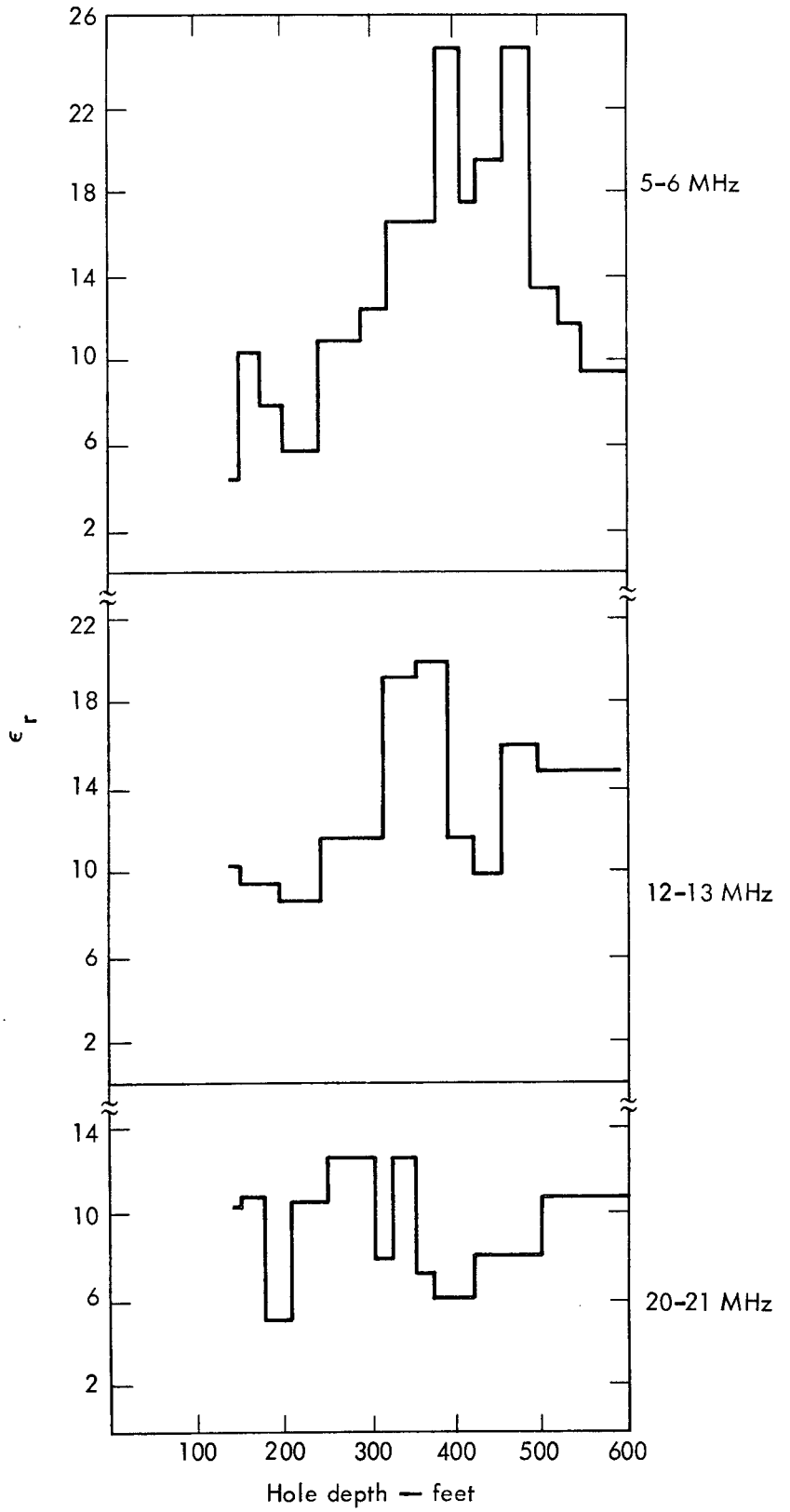

Fig. 28. Variation of ϵ_r with depth and frequency.

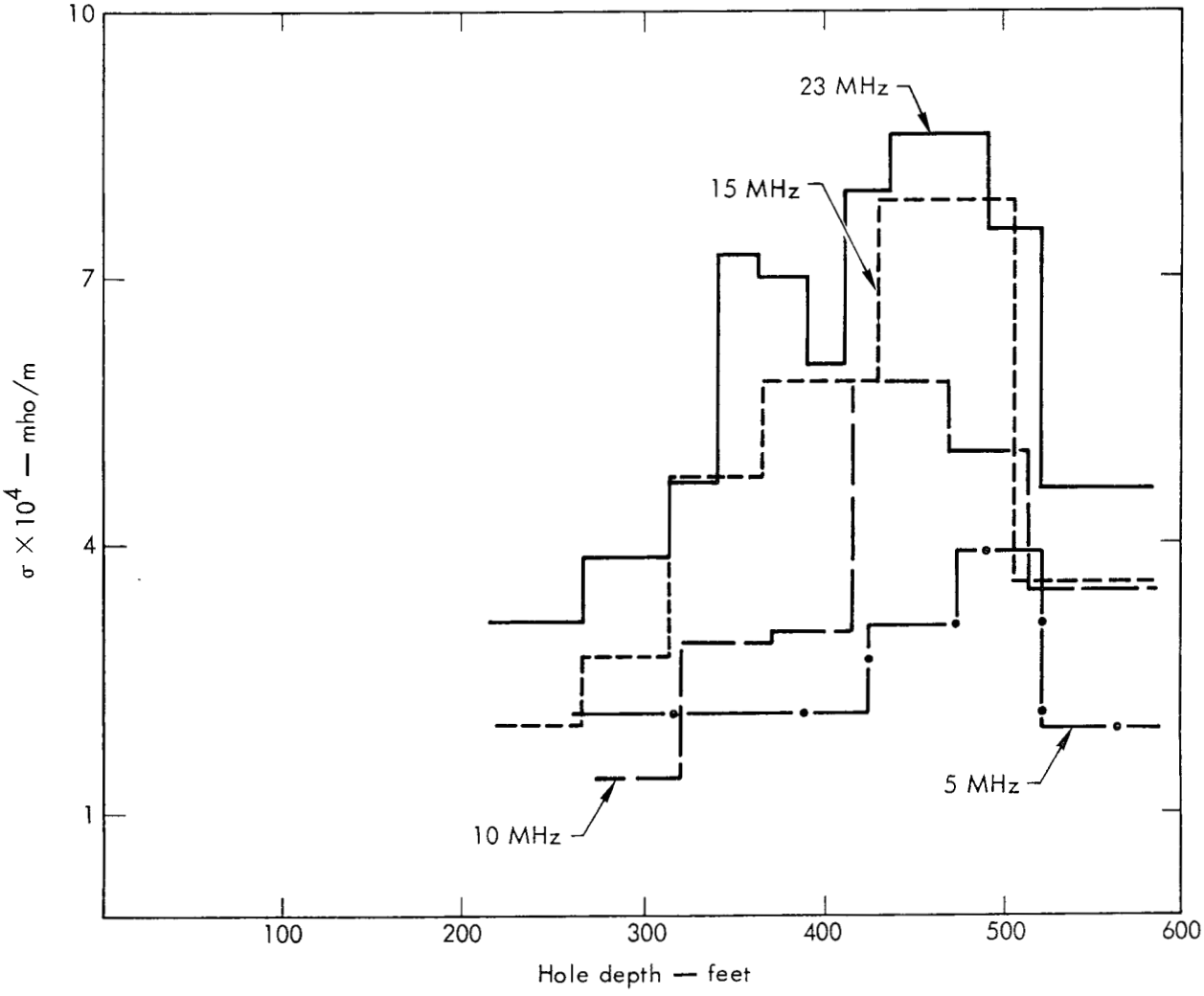

Fig. 29. Variation of σ with depth and frequency.

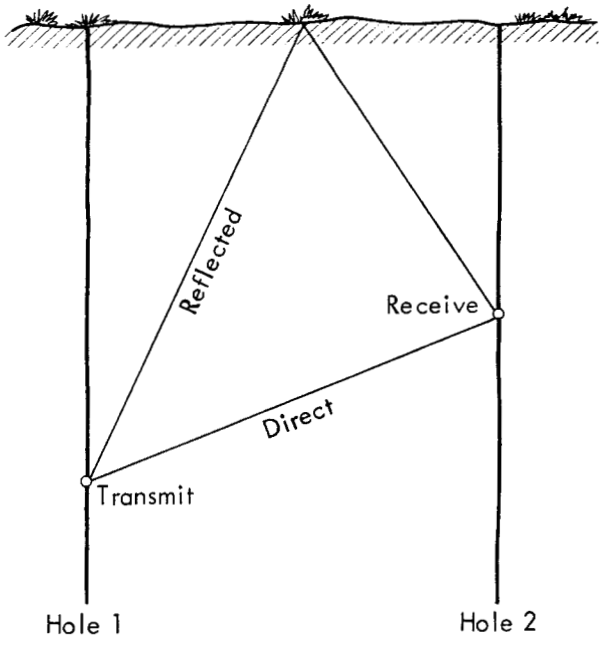

depth of transmitter and receiver. This is quite evident in the experimental data shown in Fig. 31. Note that the closer the transmitter and receiver are to the electrical discontinuity, the wider the notching behavior. By using a value of

Fig. 30. An electrical parameter discontinuity in hole-to hole transmissions.

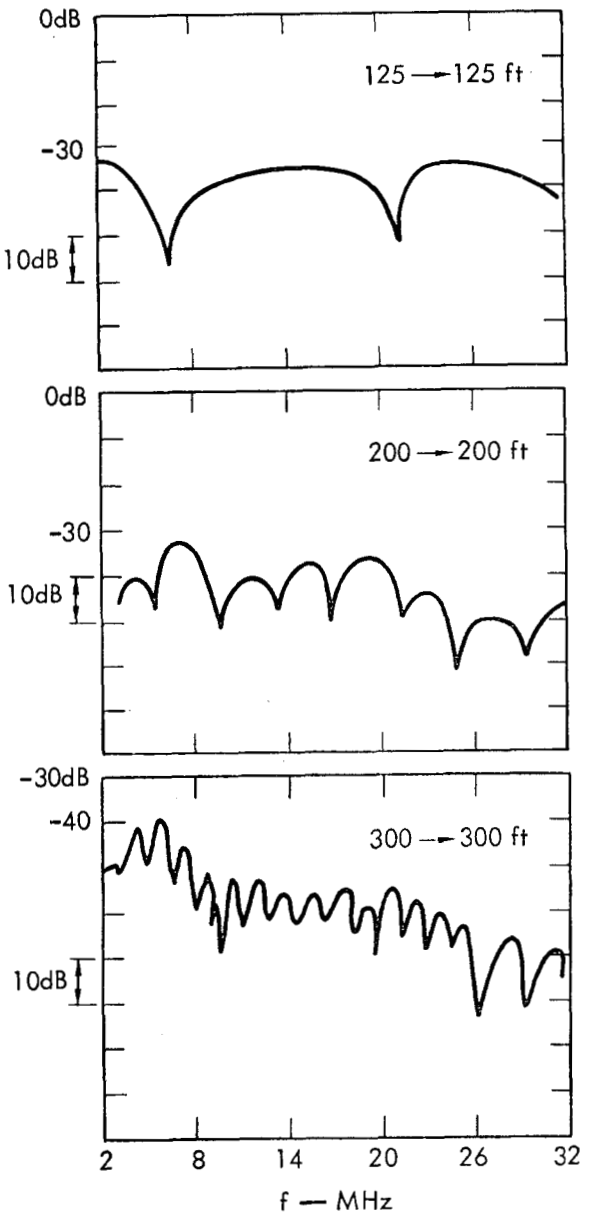

ϵ_r, the notch width, and the separation between transmitter and receiver, one can determine where the transmitter and receiver are relative to the ground-air interface. This procedure can also be used to locate subsurface anomalies. A variation on the procedure using surface-to-hole transmissions can also be used.

Fig. 31. Variation of frequency notching width with depth.

Acknowledgments

Various members of the Lawrence Livermore Laboratory Electromagnetics and Systems Research Group have provided inputs in the preparation of this report. These members are E. F. Laine, D. L. Lager, E. K. Miller and A. J. Poggio.

References

OVERVIEW REFERENCES

1. H. Fine, "An Effective Ground Conductivity Map for Continental United States," Proc. IRE 42, 1405 (1954).
2. L. A. Ames, J. W. Frazier and A. S. Orange, "Geological & Geophysical Considerations in Radio Propagation Through the Earth's Crust," IEEE Trans. Antennas and Propagation AP-11, 369 (1963).
3. G. V. Keller, "Electrical Properties in the Deep Crust," IEEE Trans. Antennas and Propagation AP-11, 344 (1963).
4. Reference Data for Radio Engineers, 5th Ed. Intern. Tel. & Teleg. Corp. (Howard W. Sams Inc., N.Y. 1968).
5. A. M. Ryazantsev and A. V. Shabel'nikov, "Propagation of Radio Waves Through the Earth's Crust (A Review)," Radio Engineering and Electron. Physics 10, 1643 (1965).
6. G. V. Keller and F. C. Frischknecht, Electrical Methods in Geophysical Prospecting (Pergamon Press, New York, 1966).
7. E. I. Parkhomenko, Electrical Properties of Rocks (Plenum Publ. Corp., New York, 1967).
8. Ye L. Feynberg, The Propagation of Radio Waves Along the Surface of the Earth, AD 660951, March 1967.
9. L. L. Vanyan, Electromagnetic Depth Soundings (Plenum Publ. Corp., New York, 1967).
10. H. E. Bussey, "Measurement of RF Properties of Materials—A Survey," Proc. IEEE 114, 1046 (1967).
11. P. David and J. Voge, Propagation of Waves (Pergamon Press, New York, 1969).
12. V. S. Yakupov, S. G. Byalobzkeskiy, Sh. Sh. Gassanov, L. I. Izmaylov and G. V. Lapshin, "Maps of the Electric Conductivity of Rocks in the Permafrost Zone of the Northeastern Part of the USSR," Acad. Sci., USSR Izvestiya Phys. Solid Earth, No. 8 p. 537 (1969).
13. J. R. Wait, Electromagnetic Waves in Stratified Media (Pergamon Press, New York, 1970).
14. J. R. Wait, Ed., Electromagnetic Probing in Geophysics (Golem Press, Boulder, Colo., 1971).
15. J. G. Heacock, Ed., The Structure and Physical Properties of the Earth's Crust, Geophys. Monograph 14, Am. Geophys. Union, Washington, D.C., 1971.
16. J. T. deBettencourt, D. Davidson and J. R. Wait, On Radio Methods of Measuring Earth Conductivity, Report of IEEE Wave Propagation Committee's Subcommittee on Earth Conductivity Measurements, March 1, 1972.

17. L. S. Collett and T. J. Katsube, "Electrical Parameters of Rocks in Developing Geophysical Techniques " Geophysics 38, 76 (1973).

LABORATORY MEASUREMENT REFERENCES

18. A. R. von Hipple, Ed., Dielectric Materials and Applications (John Wiley and Sons, New York, 1954).
19. B. F. Howell, Jr., and P. H. Licastro, "Dielectric Behavior of Rocks and Minerals," Am. Mineralogist 46, 269 (1961).
20. R. Abbato, "Dielectric Constant Measurements Using RCS Data," Proc. IEEE 112, 1095 (1965).
21. J. H. Scott, R. D. Carroll and D. R. Cunningham, "Dielectric Constant and Electrical Conductivity Measurements of Moist Rock: A New Laboratory Method," J. Geophys. Res. 72(20), 5101 (1967).
22. T. Yoshino, "The Reflection Properties of Radio Waves on the Ice Cap," IEEE Trans. Antennas Propagation AP-15, 542 (1967).
23. K. Iizuka and T. Sugimoto, "Measurement of the Dielectric Properties of Soft Materials With High Loss and High Permittivity in a Parallel Plate Region," Proc. IEEE 114, 1219 (1967).
24. D. C. Auth, W. G. Mayer and W. J. Thaler, "A Light Diffraction Technique for Measuring Dielectric Constants at Microwave Frequencies," Proc. IEEE 116, 96 (1969).
25. J. S. Yu and L. J. Peters, Jr., "Measurement of Constitutive Parameters Using the Mie Solution of a Scattering Sphere," Proc. IEEE 117, 876 (1970).
26. J. C. Cook, "RF Electrical Properties of Bituminous Coal Samples," Geophysics 35, 1079 (1970).
27. A. S. Khalafalla and J. M. Viner, Rock Dielectrometry at Mega- and Giga-Hertz Frequencies, 1973 URSI Meeting, Boulder, Colorado, August 1973.
28. P. Hoekstra and A. Delaney, The Dielectric Properties of Soils at UHF and Microwave Frequencies, 1973 URSI Meeting, Boulder, Colorado, August 1973.
29. A. W. Straiton, B. M. Fannin and J. W. Perry, Measurement of Complex Dielectric Constant of Ice Fogs Using a Fabry-Perot Resonant Cavity, 1973 URSI Meeting, Boulder, Colorado, August 1973.

IN SITU SURFACE MEASUREMENT REFERENCES

30. K. A. Norton, "The Propagation of Radio Waves Over the Earth and in the Atmosphere," Part I, Proc. IRE 24, 1367 (1936), and Part II, Proc. IRE 25, 1203 (1937).

31. G. Millington, "Ground-Wave Propagation Over an Inhomogeneous Smooth Earth," Proc. I.E.E. (London) 96, Part III, 53 (1949).
32. M. A. H. El-Said, "A New Method for the Measurement of the Average Dielectric Constant of the Underground Medium on Site," IEEE Trans. Antennas Propagation AP-4, 601 (1956).
33. K. E. Eliassen, "A Survey of Ground Conductivity and Dielectric Constant in Norway Within the Frequency Range 0.2-10 Mc/s," Geofys. Publikasjoner 19 (1957).
34. J. R. Wait and A. M. Conda, "On the Measurement of Ground Conductivity at VLF," IEEE Trans. Antennas Propagation AP-6, 273 (1958).
35. G. S. Saran and G. Held, "Field Strength Measurements in Fresh Water," J. Res. NBS, D. Radio Propagation 64D, 435 (1960).
36. S. W. Maley, "A Method for the Measurement of the Parameters of a Two-Layer Stratified Earth," IEEE Trans. Antennas Propagation AP-11, 366 (1963).
37. J. R. Wait and L. C. Walters, "Curves for Ground Wave Propagation Over Mixed Land and Sea Paths," IEEE Trans. Antennas Propagation AP-11, 38 (1963).
38. S. Krevsky, "HF and VHF Radio Wave Attenuation Through Jungle and Woods," IEEE Trans. Antennas Propagation AP-11, 506 (1963).
39. R. J. King, "Crossed-Dipole Method of Measuring Wave Tilt," Radio Sci. 3, 345 (1968).
40. A. W. Biggs, "Terrin Influences on Effective Ground Conductivity," IEEE Trans. Geosci. Electron. GE-8, 106 (1970).
41. K. P. Spies and J. R. Wait, "Determining Electrical Ground Constants from the Mutual Impedance of Small Coplanar Loops," IEEE Trans. Antennas Propagation AP-20, 501 (1972).
42. J. Lytle, E. Laine and D. Lager, "Determination of the In Situ Conductivity and Dielectric Constant Via the Two-Loop Method Using Swept Frequency Excitation," Lawrence Livermore Laboratory, Rept. UCRL-51266 (1972).
43. D. McNeill and P. Hoekstra, "In-Situ Measurements on the Conductivity and Surface Impedance of Sea Ice at VLF," Radio Sci. 8, 23 (1973).
44. S. H. Ward, "Gross Estimates of the Conductivity, Dielectric Constant, and Magnetic Permeability Distributions in the Moon," Radio Sci. 4, 117 (1969).
45. K. R. Cook and W. P. Waite, Measurement of Dielectric Constant and Soil Moisture with a 4-25 GHz Reflectometer, 1973 URSI Meeting, Boulder, Colorado, August 1973.
46. P. Hoekstra, The Electrical Resistivity Profile of Permafrost, 1973 URSI Meeting, Boulder, Colorado, August 1973.
47. G. Simmons for the SEP TEAM, Electromagnetic Probing of the Moon, 1973 G-AP Intern. Symp., Boulder, Colorado, August 1973.
48. H. E. Bussey, Dielectric Constant Measurements of the Earth, 1973 URSI Meeting, Boulder, Colorado, August 1973.

49. E. J. Kirscether, "Ground Constant Measurements Using a Section of Balanced Two-Wire Transmission Line," IRE Trans. Antennas Propagation AP-8, 307 (1960).

50. F. Segesmen, S. Soloway and M. Watson, "Well-Logging—The Exploration of Subsurface Geology," Proc. IRE 50, 2227 (1962).

51. J. T. deBettencourt and J. W. Frazier, "Rock Electrical Characteristics Deduced From Depth Attenuation Rates (in Drill Holes)," IEEE Trans. Antennas and Propagation AP-11, 358 (1963).

52. J. Carolan, Jr., and J. T. deBettencourt, "Radio Waves in Rock Near Overburden-Rock Interface," IEEE Trans. Antennas Propagation AP-11 336 (1963).

53. C. K. H. Tsao and J. T. deBettencourt, "Measurement of the Phase Constant for Rock-Propagated Radio Signals," IEEE Trans. Comm. Tech. COM-15, 592 (1967).

54. C. K. H. Tsao and J. T. deBettencourt, "Measurement of Conductivity with Electrically Short Probe," IEEE Trans. Instr. and Measurement IM-16, 242 (1967).

55. C. K. H. Tsao and J. T. deBettencourt, "Subsurface Radio Propagation Experiments," Radio Sci. 3, 1039 (1968).

56. V. N. Nikitina and B. S. Enenshteyn, "Determination of the Electric Properties of Rock in Its Natural State in the Crystalline Basement," Acad. Sci., USSR Izvestiya, Phys. Solid Earth, No. 12, p. 748 (1968).

57. R. N. Grubb and J. R. Wait, "In Situ Measurements on the Complex Propagation Constant in Rocks for Frequencies From 1 to 10 MHz," Electronics Letters 7, 506 (1971).

58. J. R. Wait and J. A. Fuller, "On Radio Propagation Through Earth," IEEE Trans. Antennas Propagation AP-19, 796 (1971).

59. J. A. Fuller and J. R. Wait, "EM Coupling of Co-Axial and Co-Planar Loops in Uniform Dissipative Media," Proc. IEEE 60, 993 (1972).

60. J. A. Fuller and J. R. Wait, Mutual Electromagnetic Coupling of Coaxial Loops in a Borehole, NOAA Internal Rept., 1972.

61. J. C. Rogers and I. C. Peden, The VLF Permittivity of Deep Antarctic Ice Measured In Situ With an Electrically Short Dipole Probe, 1973 G-AP Intern. Symp., Boulder, Colorado, August 1973.

62. R. J. Lytle, The Yosemite Experiments: HF Propagation Through Rock, 1973 URSI Meeting, Boulder, Colorado, August 1973.

63. R. J. Lytle, E. F. Laine, D. L. Lager and J. T. Okada, The Lisbourne Experiments: HF Propagation Through Permafrost Rock, Lawrence Livermore Laboratory, Rept. UCRL-51474 (1973).

MODELING MEASUREMENT REFERENCES

64. L. S. Taylor, "Dielectric Properties of Mixtures," IEEE Trans. Antennas Propagation AP-13, 943 (1965).

65. K. Iizuka, "Technique of Fabricating Inhomogeneous Mediums and the Behavior of a Dipole in Such a Medium," Proc. IEEE 114, 595 (1967).

66. K. Iizuka, "Application of an Agar-Agar Chamber for the Study of Electromagnetic Waves in an Inhomogeneous Medium," IEEE Trans. Antennas Propagation AP-20, 602 (1972).

67. A. Abul-Kassem, Experimental Investigation of the Impedance of a Horizontal Linear Antenna Above a Dissipative Homogeneous Earth, 1973 G-AP Intern. Symp., Boulder, Colorado, August 1973.

68. D. C. Pearce, W. H. Hulse, Jr., and J. W. Walker, "The Application of the Theory of Heterogeneous Dielectrics to Low Surface Area Soil Systems," IEEE Trans. Geosci. Electron. GE-11, 167 (1973).

GEOPHYSICAL PROBING AND PROFILE REFERENCES

69. M. A. H. El-Said, "Geophysical Prospecting of Underground Water in the Desert by Means of Electromagnetic Interference Fringes," Proc. IRE 44, 24 (1956).

70. W. D. Becker and C. B. Sharpe, "A Synthesis Approach to Magnetotelluric Exploration," Radio Sci. 4, 1089 (1969).

71. G. T. Inouye, H. Bernstein and R. A. Gaal, "Electromagnetic Depth Sounder," IEEE Trans. Geosci. Electron. GE-8, 336 (1970).

72. R. Mittra and D. H. Schaubert, "Study of a Remote Probing Technique for Inhomogeneous Media," Proc. IEEE 118, 1539 (1971).

73. L. Colin, Ed., Mathematics of Profile Inversion, NASA Workshop Proc., NASA TM X-62, 150, August 1972.

74. M. Mostafavi and R. Mittra, "Remote Probing of Inhomogeneous Media Using Parameter Optimization Techniques," Radio Sci. 7, 1105 (1972).

75. J. C. Cook and J. J. Wormser, "Semi-Remote Acoustic, Electric, and Thermal Sensing of Small Buried Nonmetallic Objects," IEEE Trans. Geosci. Electron. GE-11, 135 (1973).

76. P. Hoekstra and D. McNeil, "Electromagnetic Probing of Permafrost," Proc. Second Intern. Permafrost Conf., Yakatok, USSR, July 1973 (published by National Academy of Sciences).

77. V. S. Luchinonov, "Radar Sensing of Mountain Glaciers," Soviet Phys. Tech. Phys. 18, 415 (1973).

78. L. T. Dolphin, R. I. Bollen and G. N. Oetzel, An Underground Electromagnetic Sounder Experiment, 1973 URSI Meeting, Boulder, Colorado, August 1973.

79. R. Mittra, Numerical Techniques for Antennas and Electromagnetics, Chapt. 7, Inverse Scattering and Remote Probing, (to be published).

Distribution

LLL Internal Distribution

Roger E. Batzel	L-1	
J. Carothers	L-7	
L. Cleland	L-156	
W. Dickinson	L-14	
L. Germain	L-7	
G. Higgins	L-43	
F. Holzer	L-43	
J. Howard	L-47	
J. Kahn	L-41	
O. Krause	L-153	
G. Longerbeam	L-153	
H. McDonald	L-151	
E. Miller	L-156	
W. Ramsey	L-41	
B. Rubin	L-43	
J. Shearer	L-18	
D. Stephens	L-437	
G. Werth	L-13	
S. Winter	L-43	
M. Knapp	L-531	
A. Poggio	L-156	
D. Lager	L-156	
E. Laine	L-531	
C. Maninger	L-340	
M. McClelland	L-531	
E. Lafranchi	L-151	
E. Behrin	L-318	
T. Boster	L-45	
J. Lytle	L-156	
J. Brown	L-156	60
L. Wouters	L-48	
TID File		30

External Distribution

A. Dey
University of California
419 Hearst Mining Bldg
Berkeley, CA 94720

R.L. Fante
Avoc Systems Div.
210 Lowell Street
Wilmington, MA

L.B. Felsen
Polytech Institute of Brooklyn
Graduate Center
Rt. 110
Farmingdale, NY 11735

J.A. Fuller
NASA, Manned Space Flight Center
Astronics Dept.
Redstone Arsenal
Huntsville, AL 35809

R. Gabillard
Des Sciences Techniques D Lille
VER I.E.E.A.
B.P. 36 Villenivue
D'Ascq - 59 France

J. Goodwin
ARPA
1400 Wilson Blvd.
Arlington, VA 22209

P. Hansen
Naval Electronics Laboratory Center
San Diego, CA 92152

R.F. Harrington
Syracuse University
Dept. EE, Hinds Hall
Syracuse, NY 13210

W. Henry
U.S. Coast Guard (EEE63)
400 Seventh Street S.W.
Washington, D.C. 20590

P. Hoekstra
Department of the Army
U.S. Army Cold Regions Research
and Engineering Laboratory
Hanover, NH 03755

C. Abertsen
The Technical U of Denmark
Laboratory of Electromagnetic
Theory
Building 348
DK-2800
Lyngby, Denmark

D.E. Barrick
NOAA
U.S. Dept. of Commerce
Boulder, CO 80302

K.G. Balmain
University of Toronto
Dept. EE
Toronto 181, Ontario
Canada

C. Baum
AFWL
Kirtland AFB, NM 87117

A.W. Biggs
University of Kansas
Lawrence, KS 66044

External Distribution, Continued

J. Bridges
IITRI
10 West 35th
Chicago, IL 60068

C.M. Butler
Dept of Electrical Eng.
University of Mississippi
University, MS 38677

J.P. Castillo
905 Mesilla Ave. N.E.
Albuquerque, NM 87110

D.C. Chang
Dept. of Elect. Eng.
University of Colorado
Boulder, CO 80302

J.T. de Bettencourt
Raytheon Co
1415 Providence Hwy
Norwood, MA 02062

K. Iizuka
University of Toronto
Dept. EE
35 St. George Street
Toronto 5, Ontario, Canada

A. Ishimaru
University of Washington
4000 15th Ave. N.E.
Seattle, WA 98105

F.J. Kelly (code 5461)
Naval Research Lab
Washington, DC 20390

R.J. King
University of Wisconsin
Dept. EE
500 Lincoln Dr
Madison, WI 53706

E. Kopf
ARPA
Strategic Tech. Office
1400 Wilson Blvd
Arlington, VA 22209

C. Malagesi
Rome Air Development Center
Griffiss AFB, NY 13440

K.K. Mei
University of California
Dept. EE & Computer Sciences
Berkeley, CA 94720

R. Mittra
University of Illinois
Dept. of Electronics Engineering
5801 So. Ellis
Urbana, IL 61801

R.K. Moore
University of Kansas
Marvin Hall
Lawrence, KS 66044

H.F. Morrison
Engineering Ge Science
Hearst Mining Bldg
University of California
Berkeley, CA 94270

B. Olsen
Washington State University
Dept of Electrical Engineering
Pullman, WA 99163

R.H. Ott
Institute for Telecommunication
Services
Boulder, CO 80302

T.P. Quinn
Office of Naval Research
Earth Sciences Division
17th & Constitution Ave.
Washington, D.C. 20360

L.J. Ricardi
MIT Lincoln Lab
244 Wood Street
Lexington, MA 02137

J. Ruze
MIT Lincoln Laboratory
244 Wood Street
Lexington, MA 02137

F.V. Schultz
Purdue University
Lafayette, IN 47907

D. Strang
Sanders Associates Inc.
95 Canal Street
Nashua, NH 03060

J.R. Wait
Environmental Research Lab
NOAA
U.S. Dept of Commerce
Boulder, CO 80302

External Distribution, Continued

S.H. WArd
Dept. of Geological &
Geophysical Sciences
University of Utah
University St and Second So.
Salt Lake City, UT 84112

H.A. Wheeler
Wheeler Labs Inc.
Route 25A
Smithtown, NY 11787

TID-4500, UC-34
Physics General 114

VRM/1h/eap/1g